

Planar Conformal Mappings of Piecewise Flat Surfaces

Philip L. Bowers and Monica K. Hurdal

Department of Mathematics, The Florida State University, Tallahassee, FL 32306, USA.

bowers@math.fsu.edu

mhurdal@math.fsu.edu

Introduction[†]

There is a rich literature in the theory of circle packings on geometric surfaces that from the beginning has exposed intimate connections to the approximation of conformal mappings. Indeed, one of the first publications in the subject, Rodin and Sullivan's 1987 paper [10], provides a proof of the convergence of a circle packing scheme proposed by Bill Thurston for approximating the Riemann mapping of an arbitrary proper simply-connected domain in \mathbb{C} to the unit disk. Bowers and Stephenson's work in [4], which explains how to apply the Thurston scheme on nonplanar surfaces, may be viewed as a far reaching generalization of his scheme to the setting of arbitrary equilateral surfaces. Further, in [4] Bowers and Stephenson propose a method for uniformizing more general piecewise flat surfaces that necessitates a truly new ingredient, namely, that of inversive distance packings. This inversive distance scheme was introduced in a very preliminary way in [4] with some comments on the difficulty involved in proving that it produces convergence to a conformal map. Even with these difficulties, the scheme has been encoded in Stephenson's packing software `CirclePack` and, though all the theoretical ingredients for proving convergence are not in place, it seems to work well in practice. This paper may be viewed as a commentary on and expansion of the discussion of [4]. Our purposes are threefold. First, we carefully describe the inversive distance scheme, which is given only cursory explanation in [4]; second, we give a careful analysis of the theoretical difficulties that require resolution before conformal convergence can be proved; third, we give a gallery of examples illustrating the power of the scheme. We should note here that there are special cases (e.g., tangency or overlapping packings) where the convergence is verified, and our discussion will give a proof of convergence in those cases.

Each oriented piecewise flat surface has a natural conformal structure defined on its interior by a complex atlas with conformal charts of two types. First, each interior edge gives rise to an edge chart that isometrically maps the

[†] This work is supported by NSF grant DMS-0101329, NIH grant MH-57180 and FSU grant FYAP-2002.

interior of the two Euclidean triangles meeting along that edge to the plane, preserving orientation. Overlap maps between the intersections of two such charts are Euclidean isometries and therefore conformal. Second, each interior vertex gives rise to a vertex chart that uses a power map defined on a small open neighborhood of the vertex to rescale an angle sum Θ different from 2π to one equal to 2π . The vertex charts are chosen to have pairwise disjoint domains and the local form of the chart map is the power map $z \mapsto z^{2\pi/\Theta}$. The overlap mapping between any edge chart and vertex chart is conformal as the vertex, where the derivative is zero, is not in the overlap. In this way any orientable piecewise flat surface becomes a Riemann surface. Notice that though there are in general cone points at the vertices in a piecewise flat surface, these are singularities of the piecewise Euclidean metric only and not singularities of the conformal structure. Indeed, the total angle sum at each vertex given by the conformal structure is 2π and the Euclidean angle α between two arcs emanating from a vertex is measured as $2\pi \frac{\alpha}{\Theta}$ in the conformal structure. The conformal structure thus measures the “market share” of the angle α with respect to the total Euclidean angle Θ .

Though the inversive distance scheme for conformal mapping may be presented in the full generality of arbitrary piecewise flat surfaces, of arbitrary genus with an arbitrary number of boundary components, we have chosen to restrict our attention to the simply connected case so as to illuminate the essential features of the algorithm and so that we may discuss the details of the proof of convergence without the added difficulty of having to work with moduli spaces. In fact, we will consider piecewise flat quadrilaterals and ask for a method to conformally map them to rectangles.

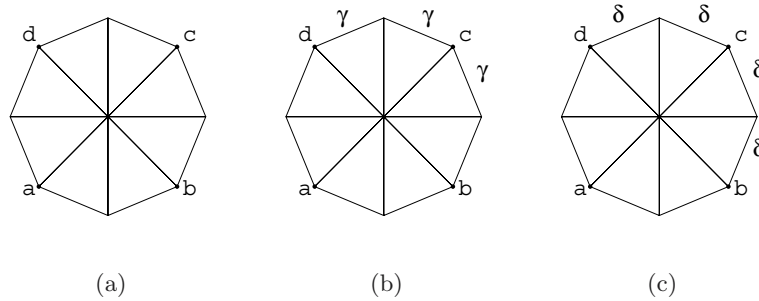


Fig. 1. Three piecewise flat conformal quadrilaterals.

Perhaps an example will help illustrate the problem the algorithm addresses. Consider the simple triangulation K of a topological quadrilateral with eight faces with a common central vertex and four distinguished bound-

ary vertices a , b , c , and d as in Fig. 1. There are many ways to define a metric on K making each face a flat Euclidean triangle. Three examples are indicated in Fig. 1 where each side is given unit length, except for the sides labeled with γ and δ , which are given side lengths $\gamma = 0.3473$ and $\delta = 0.2611$. These examples are discussed in greater detail in Section 5, but for now realize that these labels encode a piecewise flat metric on K by identifying the faces with Euclidean triangles of side lengths given by the edge labels. This in turn produces three different conformal structures on K that each realizes K as a conformal quadrilateral. By standard theorems on conformal mapping, any conformal quadrilateral maps conformally to a Euclidean rectangle unique up to scaling. Approximations to this conformal mapping in each case are indicated in Fig. 2, where we see approximations to the image triangulations under the conformal mapping to a rectangle. Note that the first and third rectangles of Fig. 2 are both squares, but the conformally correct shapes of the faces in the two examples are different, and the conformal modulus of the second is approximately $\mu = 1.2031$.

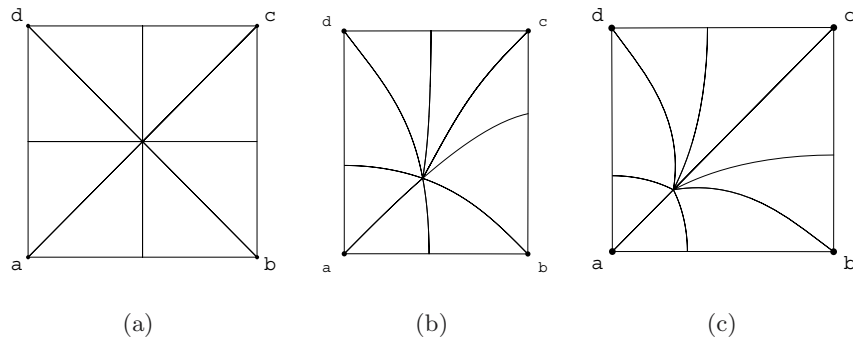


Fig. 2. Uniformizations of quadrilaterals from Fig. 1.

Complete proofs for convergence of the scheme in the more specialized setting of equilateral surfaces, where each edge has unit length and each face is identified with a unit equilateral triangle, are found in [4]. The original motivation for developing the scheme of [4] was to construct fundamental domains for the equilateral surfaces that arise in Grothendieck’s theory of dessins d’enfants and to approximate their associated Belyı̄ maps. Since then, Hurdal *et al* [7] have adopted this method to construct flat mappings of surfaces in \mathbb{R}^3 and have applied the method to obtain flat mappings of the human brain, which is of current interest in the neuroscience community. The desire to obtain better conformal integrity in these brain mappings has inspired us to investigate further this preliminary suggestion in [4] that a modification of their scheme using inversive distance packings could be used to build con-

formal mappings in this piecewise flat—as opposed to piecewise equilateral—setting. Stephenson’s software `CirclePack` was used for the brain mappings of [7] as well as for calculating and rendering our examples. We note here that we do not present the circle packing algorithm used in `CirclePack` to calculate the packing for given inversive distance data as this has been discussed amply in [5].

The ingredients of this conformal mapping scheme are inversive distances of circles in the Riemann sphere, circle patterns in the Riemann sphere, and hexagonal refinement. The first three sections of the paper are centered around these three respective themes. We find that many mathematicians, even those who specialize in complex analysis and conformal geometry, are not familiar with the inversive distance between pairs of circles in the Riemann sphere. In Section 1, we present an inversive distance primer and prove some results about the conformal placement of circles in the Riemann sphere. In Section 2, we review the basics of piecewise flat structures on surfaces and introduce circle patterns with inversive distances encoded along edges. These patterns, generalizations of circle packings where edges encode tangencies, have been studied in the case where neighboring circles overlap with some angle between 0 and $\pi/2$. Bowers and Stephenson [4] introduced the notion of circle patterns where neighboring circles may not overlap, but where they do satisfy *á priori* inversive distance requirements. We emphasize again that the theoretical underpinnings of this topic are not entirely in place and are a matter of current research by Bowers, Stephenson, Hurdal, and others, but the good news is that the algorithm seems to work well in practice. This iterative algorithm for producing a sequence of patterns that are hoped to approximate more and more closely the desired conformal mapping is presented in Section 3, where hexagonal refinements are introduced. The difficulties in the proof of convergence to the desired conformal mapping are discussed in Section 4. We detail three main theoretical problems that must be addressed for a complete resolution of the question of convergence to a conformal map, and we prove convergence under the assumption that these problems have been resolved. Section 5 presents a gallery of examples that illustrate the algorithm by approximating conformal mappings to rectangles of conformal quadrilaterals that arise from piecewise flat metrics on topological disks, as in the examples of this introduction. This allows us to approximate the conformal moduli of quadrilaterals that arise from piecewise flat metrics, and to view the conformally correct shapes of the faces of the triangulation after mapping to the plane. We shall point out how well the algorithm works in practice, producing image triangulations with exactly the expected properties. Finally, Section 6 discusses practical implementation issues in applications, and computational and theoretical issues surrounding these.

1 An Inversive Distance Primer

The inversive distance between two oriented circles in the Riemann sphere $\widehat{\mathbb{C}}$ is a conformal invariant of the location of the circles in the sphere and their relative orientations; see [1]. Indeed, given oriented circle pairs C_1, C_2 and C'_1, C'_2 of $\widehat{\mathbb{C}}$, there exists a Möbius transformation T of the Riemann sphere with $T(C_i) = C'_i$ for $i = 1, 2$, respecting their relative orientations, if and only if the inversive distance between C_1 and C_2 equals that between C'_1 and C'_2 . An oriented circle C is the boundary of a unique open disk \overline{C} , called the interior of C , that lies to the left of C as C is traversed in the direction of its orientation. The precise definition of inversive distance may be stated elegantly with the aid of cross ratios and circle interiors.

Definition 1. *Let C_1 and C_2 be oriented circles in the Riemann sphere $\widehat{\mathbb{C}}$ bounding the respective disks \overline{C}_1 and \overline{C}_2 , and let D be any oriented circle mutually orthogonal to C_1 and C_2 . Denote the points of intersection of D with C_1 as z_1, z_2 ordered so that the oriented subarc of D from z_1 to z_2 lies in the disk \overline{C}_1 . Similarly denote the ordered points of intersection of D with C_2 as w_1, w_2 . The inversive distance between C_1 and C_2 , denoted as $\text{InvDist}(C_1, C_2)$, is defined in terms of the cross ratio*

$$[z_1, z_2; w_1, w_2] = \frac{(z_1 - w_1)(z_2 - w_2)}{(z_1 - z_2)(w_1 - w_2)}$$

by

$$\text{InvDist}(C_1, C_2) = 2[z_1, z_2; w_1, w_2] - 1.$$

Recall that cross ratios of ordered 4-tuples of points in $\widehat{\mathbb{C}}$ are invariant under Möbius transformations. This implies that which circle orthogonal to both C_1 and C_2 is used in the definition is irrelevant as a Möbius transformation that setwise fixes C_1 and C_2 can be used to move any one orthogonal circle to another. Also, which one of the two orientations on the orthogonal circle D is used is irrelevant as the cross ratio satisfies $[z_1, z_2; w_1, w_2] = [z_2, z_1; w_2, w_1]$. This equation also shows that the inversive distance is preserved when the orientation of both circles is reversed so that it is only the relative orientation of the two circles that is important for the definition. When C_1 and C_2 overlap, the oriented angle of overlap may be defined unambiguously as the angle between the tangents to the circles at a point of overlap formed by one tangent pointing along the orientation of its parent circle and the other pointing against the orientation of its parent circle. We distinguish six different ways that two circles may overlap and describe the inversive distance in each case.

1.1 Six Cases

The inversive distance is always a real number since the cross ratio of four points that lie on a circle is always real. The way to dissect the inversive distance is through the auxiliary function

$$T(z) = 2[z_1, z_2; z, w_2] - 1 = 2 \frac{(z_1 - z)(z_2 - w_2)}{(z_1 - z_2)(z - w_2)} - 1,$$

which is a Möbius transformation that takes the triple z_1, z_2, w_2 to the triple $-1, 1, \infty$. The function T takes the orthogonal circle D to the real line, the circle C_1 to the unit circle centered at the origin, and the circle C_2 to the vertical line orthogonal to the real axis at the point $T(w_1)$; see Fig. 3. Notice that $\text{InvDist}(C_1, C_2) = T(w_1)$ may take on any real value and we distinguish the six cases according to the two relative orientations for each of the three possibilities for intersection of C_1 with C_2 . Fig. 3 provides a snapshot of all the possibilities labeled according to whether the orientations are aligned or opposite, and whether the intersection consists of none, one, or two points.

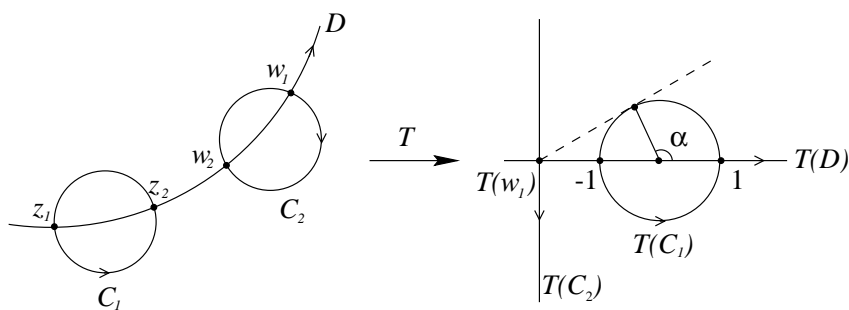
Figs. 3(a) and 3(b) illustrate the possibilities for disjoint circles. If the orientations are opposite, the inversive distance is in the range from $-\infty$ to -1 exclusive, and if aligned, in the range from $+1$ to $+\infty$ exclusive. Figs. 3(c) and 3(d) illustrate those for tangent circles where the inversive distance is ± 1 depending on relative orientation. Figs. 3(e) and 3(f) illustrate those for intersecting circles where the inversive distance is between -1 and 0 for intersection angles between π and $\pi/2$ and between 0 and $+1$ for angles between $\pi/2$ and 0 . Referring to the angle labels in Fig. 3, we may read off the inversive distances as

$$\text{InvDist}(C_1, C_2) = \sec \alpha$$

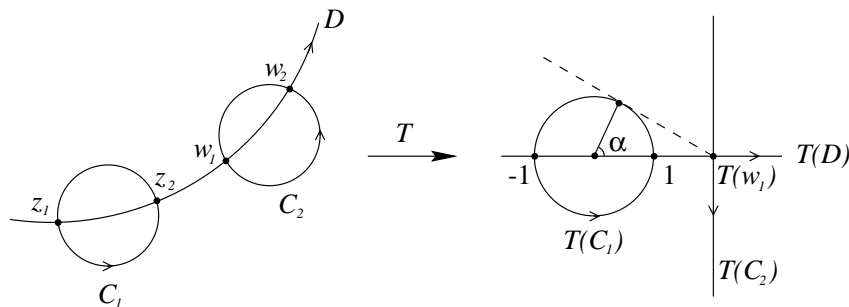
for disjoint circles, where α is the indicated angle, and

$$\text{InvDist}(C_1, C_2) = \cos \alpha$$

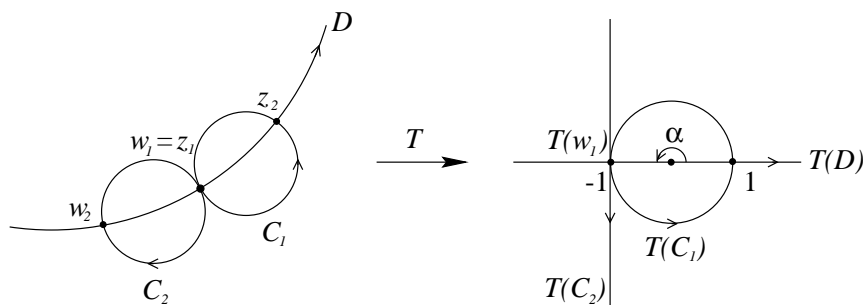
for intersecting circles, where α is the oriented angle of intersection of C_1 with C_2 . Notice for intersecting circles, since the overlap angle α may be determined without regard to the normalizing transformation T , the inversive distance has an immediate, easily understood meaning. One can look at two overlapping circle pairs and estimate whether they are Möbius equivalent, a task of great difficulty for disjoint circle pairs. For those with a finely developed intuition for hyperbolic space and the Poincaré extensions of Möbius transformations, there is a more geometric understanding of inversive distance available.



(a) Disjoint circles, opposite orientations.

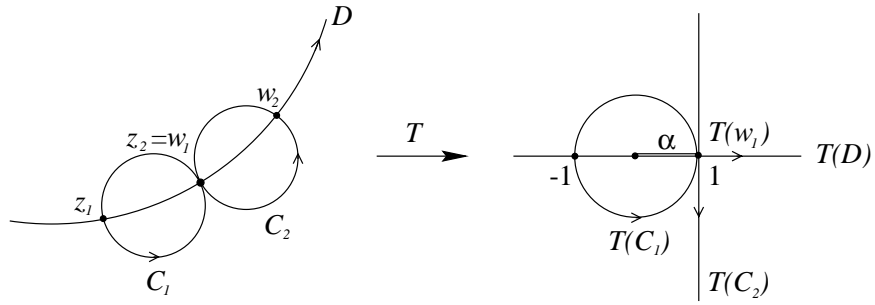


(b) Disjoint circles, aligned orientations.

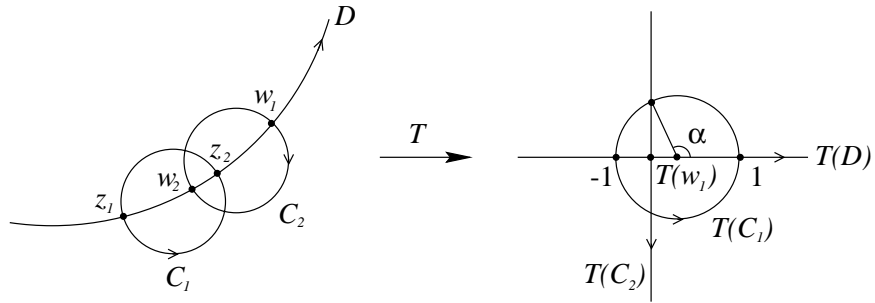


(c) Tangent circles, opposite orientations.

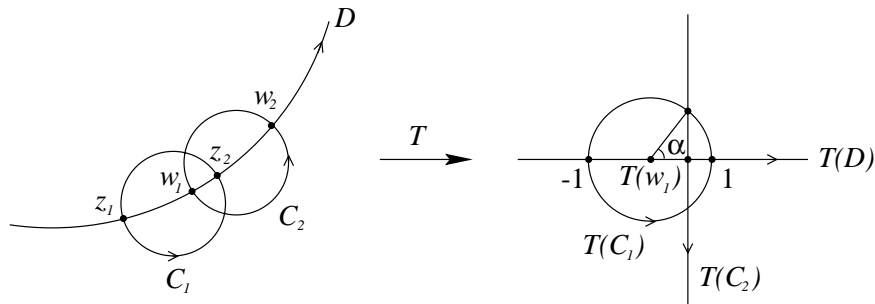
Fig. 3. Three of six ways that two circles overlap. Here, $T(z_1) = -1, T(z_2) = 1$.



(d) Tangent circles, aligned orientations.



(e) Intersecting circles, opposite orientations.



(f) Intersecting circles, aligned orientations.

Fig. 3. Remaining three ways that two circles overlap. Here, $T(z_1) = -1, T(z_2) = 1$.

1.2 An Alternate Description in Terms of Hyperbolic Geometry

Notice that if the orientation of only one member of a circle pair is reversed, the inversive distance merely changes sign. This follows from the immediate relation $[z_1, z_2; w_2, w_1] = 1 - [z_1, z_2; w_1, w_2]$. We therefore define

Definition 2. *The absolute inversive distance between any pair of unoriented circles is the absolute value of the inversive distance between the two circles when given either relative orientation. We use the same notation, $\text{InvDist}(C_1, C_2)$, for the absolute inversive distance between unoriented circles C_1 and C_2 .*

It is clear then that there is a Möbius transformation taking an unoriented circle pair C_1, C_2 to another unoriented pair C'_1, C'_2 if and only if their absolute inversive distances agree. When C_1 and C_2 overlap with acute angle α the absolute inversive distance is $\cos \alpha$ and when they are tangent it takes the value 1. In this subsection our aim is to expose a geometric understanding of the absolute inversive distance between two disjoint circles in terms of hyperbolic geometry. This is a great intuitive aid for understanding inversive distances between disjoint circles. Toward this end assume C_1 and C_2 are disjoint and by appropriate choices of orientation map via T so that $T(C_1)$ is the unit circle and $T(C_2)$ is the vertical line through the point $\Delta = \text{InvDist}(C_1, C_2) > 1$. Consider the extended complex plane as the sphere at infinity for the hyperbolic 3-space realized as the upper half-space model with metric $ds = |dx|/x_3$ on $\mathbb{H}^3 = \{x = (x_1, x_2, x_3) : x_3 > 0\}$. The Poincaré extension of T , denoted \tilde{T} , is an isometry of \mathbb{H}^3 . The circle C_1 bounds a hyperbolic plane P_1 in \mathbb{H}^3 that is realized as the upper hemisphere of the sphere in \mathbb{R}^3 with the same Euclidean center and radius as C_1 , and similarly C_2 bounds the hyperbolic plane P_2 . We calculate the hyperbolic distance δ between the planes P_1 and P_2 .

First, since \tilde{T} is an isometry, we work with $\tilde{T}(P_1)$, which is the upper hemisphere of the unit sphere in \mathbb{R}^3 , and with $\tilde{T}(P_2)$, which is the vertical half plane $\{x \in \mathbb{H}^3 : x_1 = \Delta\}$. There is a unique geodesic segment Σ in \mathbb{H}^3 meeting both $\tilde{T}(P_1)$ and $\tilde{T}(P_2)$ orthogonally at the respective points A and B . This geodesic segment lies on the circle in the vertical x_1x_3 -plane that is mutually orthogonal to $\tilde{T}(P_1)$, $\tilde{T}(P_2)$, and to the x_1 -axis; see Fig. 4. Elementary geometry shows this circle to be centered at the point $(\Delta, 0, 0)$ and of Euclidean radius $\sqrt{\Delta^2 - 1}$, and the points A and B to be given by $A = (\cos \sec^{-1} \Delta, 0, \sin \sec^{-1} \Delta)$ and $B = (\Delta, 0, \sqrt{\Delta^2 - 1})$. A calculation of the hyperbolic length of Σ by integrating the line element $ds = |dx|/x_3$ along Σ from A to B gives the value of δ as

$$\delta = \ln \left| \Delta + \sqrt{\Delta^2 - 1} \right| = \cosh^{-1} \Delta.$$

This proves that the absolute inversive distance between C_1 and C_2 is precisely the hyperbolic cosine of the hyperbolic distance between the planes P_1

and P_2 bounded by C_1 and C_2 . Experience with this understanding of inversive distance for disjoint circles coupled with the fact that Poincaré extensions of Möbius transformations are isometries of \mathbb{H}^3 has proved invaluable in our research, particularly for gaining intuition in working with disjoint circle patterns.

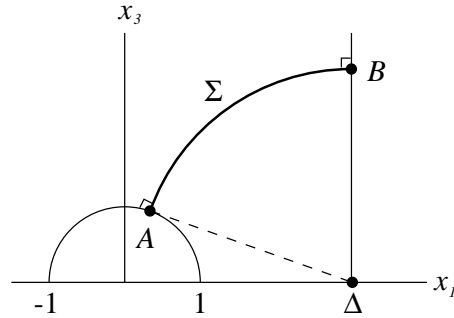


Fig. 4. The hyperbolic length of Σ is $\cosh^{-1} \Delta$.

1.3 A Euclidean Formula

The simplest formula for the absolute inversive distance between two circles in the complex plane is the one that the algorithm for conformal flattening uses. Though simple, it is not at all transparent that it should yield a Möbius invariant for the placement of two circles in the plane. We leave it as an exercise to verify that if C_i is the circle in the complex plane \mathbb{C} centered at a_i of radius R_i , for $i = 1, 2$, then the absolute inversive distance is given by

$$\text{InvDist}(C_1, C_2) = \left| \frac{R_1^2 + R_2^2 - |a_1 - a_2|^2}{2R_1R_2} \right|. \quad (1)$$

2 Piecewise Flat Surfaces and Circle Packings

A *combinatorial quadrilateral* is an abstract oriented simplicial 2-complex K that triangulates a closed topological disk with four distinguished boundary vertices $\{a, b, c, d\}$ ordered respecting the boundary orientation. The sets of vertices, edges, and faces of K are denoted respectively as \mathbf{V} , \mathbf{E} , and \mathbf{F} . A *piecewise flat structure* for K is determined by an *edge length function* $|\cdot|: \mathbf{E} \rightarrow (0, \infty)$ that satisfies the triangle inequality condition, namely, that for every three edges e_1, e_2, e_3 that bound a face of K , the inequality

$$|e_1| \leq |e_2| + |e_3|$$

holds. An edge length function $|\cdot|$ for K determines a piecewise Euclidean metric by assigning the length $|e|$ to each edge e of K and identifying each face $\langle v_1, v_2, v_3 \rangle$ with a flat Euclidean triangle of edge lengths $|e_i|$, where the edge $e_i = \langle v_j, v_k \rangle$ and $\{i, j, k\} = \{1, 2, 3\}$. The resulting piecewise Euclidean metric space is denoted as $|K|$ and, as explained in the introduction, carries the structure of a Riemann surface. Each interior vertex of K is a cone point singularity for the piecewise Euclidean metric but is not a singularity of the conformal structure. Our aim is to describe a scheme for approximating the conformal mapping of $|K|$ to a rectangle that maps the four distinguished boundary vertices to the four corners of the rectangle. Of course we do not have a candidate for the target rectangle since we do not know the modulus of the conformal quadrilateral $|K|$; however, the algorithm ideally will produce a sequence of target rectangles that converges to the correct one as well as a curvilinear triangulation of the target rectangle with the combinatorics of K that shows the correct conformal shapes of the faces.

A plentiful supply of piecewise flat surfaces is available from triangular grids in \mathbb{R}^3 where we read off side lengths of edges of actual Euclidean triangles. This, though, gives but a limited supply of the piecewise flat surfaces available, as many such surfaces admit no isometric embedding in \mathbb{R}^3 , and many admit no embedding in any Euclidean space that isometrically embeds each edge as a straight Euclidean line segment.

The iterative algorithm for conformally mapping $|K|$ to a rectangle uses as seed certain inversive distance data calculated from the edge length function $|\cdot|$. This gives rise to a piecewise flat surface with inversive distance information encoded along edges by a function $\Phi: \mathbf{E} \rightarrow [0, \infty)$. We abstract this by not assuming an a priori piecewise flat structure from which the edge function Φ arises.

Definition 3. *Let $\Phi: \mathbf{E} \rightarrow [0, \infty)$ be a function on the edge set of the complex K . A circle packing for (K, Φ) is a collection*

$$\mathcal{C} = \{C_v: v \in \mathbf{V}\}$$

of circles in the plane \mathbb{C} , each oriented counterclockwise, such that the inversive distance of neighboring circles is given by Φ , i.e., $\text{InvDist}(C_u, C_v) = \Phi(\langle u, v \rangle)$ for each edge $\langle u, v \rangle$ in \mathbf{E} .

Perhaps a more descriptive term would be circle ‘pattern’, as opposed to ‘packing’, whenever the circles are disjoint. Nonetheless, we shall use the term ‘packing’ to describe a collection of circles, disjoint or not, that has a combinatorial pattern encoded in a complex K governing the placement of the circles in the plane. Tangency packings, which use only the combinatorial information encoded in K and not any varying inversive distance data, are used in [4] to uniformize piecewise equilateral surfaces. When the surface is piecewise flat where faces are generally not equilateral, more than the combinatorics of K must be used to build approximate conformal maps. We

now describe how the metric information of $|K|$ may be used to embellish the combinatorics of K with inversive distance data, which turns out to be sufficient for generating candidates for approximate conformal maps.

Let $|\cdot|$ be an edge length function for K and let $R: \mathbf{V} \rightarrow (0, \infty)$ be a positive function on the vertices that, for each edge $\langle u, v \rangle$, satisfies the condition

$$R(u)^2 + R(v)^2 \leq |\langle u, v \rangle|^2. \quad (2)$$

This inequality guarantees that if the edge $e = \langle u, v \rangle$ is drawn in the plane as a segment of length $|e|$, and circles C_u and C_v both oriented counterclockwise of respective radii $R(u)$ and $R(v)$ are centered at the vertices of e , then the oriented overlap, if the circles intersect nontrivially, is at most $\pi/2$, and the interiors, if the circles are disjoint, are also disjoint. The resulting *radius function* $R: \mathbf{V} \rightarrow (0, \infty)$ determines an inversive distance function Φ_R on the edge set by Equation 1:

$$\Phi_R(e) = \text{InvDist}(C_u, C_v) = \frac{|\langle u, v \rangle|^2 - R(u)^2 - R(v)^2}{2R(u)R(v)}. \quad (3)$$

A circle packing \mathcal{C} for (K, Φ_R) , if it exists, gives rise to a *discrete conformal mapping* of $|K|$ to the plane by mapping the vertices of K to the centers of their corresponding circles and extending affinely on the metric faces. The image of such a discrete conformal mapping is the *carrier* of the circle packing \mathcal{C} , and is the union of the triangles corresponding to the faces of K formed by connecting centers of three mutually neighboring circles by straight line segments. The circle packing \mathcal{C} is said to be *oriented* if the orientations of all of these nondegenerate triangles inherited from the orientation on K are compatible. Equivalently, \mathcal{C} is oriented if the discrete conformal mapping f is an orientation preserving map from $|K|$ to the plane. When \mathcal{C} is oriented and Φ takes values in the unit interval, this discrete conformal mapping is quasi-conformal, but it may fail to be so for general Φ values. Moreover, when \mathcal{C} is oriented, it maps the triangulation of $|K|$ to a triangulation of the image of this map, though there may be degeneracies. We describe an algorithm in the next section that produces a sequence of these discrete conformal mappings, which serve as the candidates for approximating the conformal mapping of $|K|$ to a rectangle. To force convergence we need to normalize the boundary circles in some way, and we do so by making a further demand on our circle packings that will force a rectangular shape upon the image. In general there are many different circle packings for the same data (K, Φ) . For example, in the case of tangency packings, each specification of boundary radii for the circles that correspond to boundary vertices determines a unique oriented packing with the combinatorics of K . Alternately, each specification of boundary angle sums at boundary vertices also uniquely determines an oriented packing for K . We shall call a circle packing \mathcal{C} for (K, Φ) a *rectangular packing* if it is oriented and the angle sum of the faces at a boundary

vertex in the image triangulation are all π , except at the four distinguished boundary vertices, where the angle sums are $\pi/2$. The carrier of a rectangular packing is a rectangle. Fig. 5 shows two packings and their carriers for the same piecewise flat surface $|K|$ and inversive distance data Φ ; the packing on the right is rectangular.

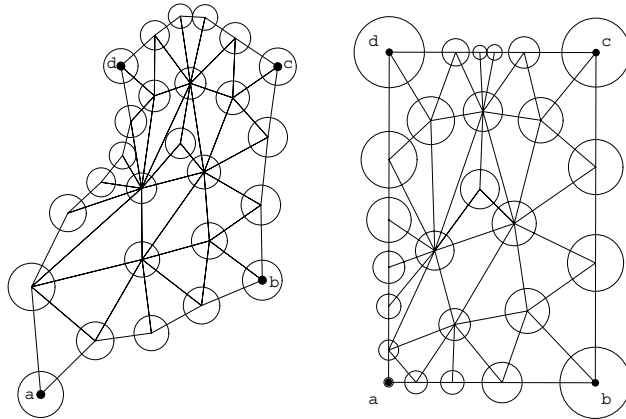


Fig. 5. Two packings for the same data (K, Φ) .

3 Hexagonal Refinement

We now fix a combinatorial quadrilateral K with an edge length function $|\cdot|$ that produces the piecewise flat conformal quadrilateral $|K|$. Let R be a constant radius function that satisfies Inequality 2 at each edge and \mathcal{C} a rectangular packing for (K, Φ_R) , where Φ_R satisfies Equation 3. It is important for proving convergence that R be a constant function. Let f be the discrete conformal mapping determined by \mathcal{C} . The seed data for our conformal mapping algorithm is the 4-tuple

$$(K_0, |\cdot|_0, R_0, \Phi_0) = (K, |\cdot|, R, \Phi_R),$$

from which we produce the mapping data

$$(\mathcal{C}_0, f_0) = (\mathcal{C}, f).$$

We think of f as the zeroth approximation to the conformal mapping that maps $|K|$ to a planar rectangle. The constant radius function may be chosen to have any positive value between 0 and $\lambda/\sqrt{2}$, where λ is the minimum of $|e|$ as e ranges over all the edges of K .

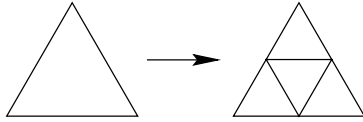


Fig. 6. Hexagonal refinement, $K \rightarrow K'$.

For better approximations we employ *hexagonal refinement*, or hex-refinement for short, which subdivides a triangle into four subtriangles as in Fig. 6; see [4]. The complex thus obtained from K by subdividing each face as in Fig. 6 is denoted as K' . There is a natural edge length function $|\cdot|'$ on K' obtained by reading off the lengths of edges obtained by placing a vertex at the midpoint of each metric edge in $|K|$ to hex-subdivide each metric face of $|K|$ into four similar copies of itself, scaled by $1/2$. Then $|K|$ and $|K'|$ are isometric and thus indistinguishable as metric spaces. If the constant radius $R' = \frac{1}{2}R$ is used for K' , the induced inversive distance function $\Phi_{R'}$ replicates on the edges of a face of K' the three inversive distances of its parent face in K . Starting then with the seed data $(K_0, |\cdot|_0, R_0, \Phi_0)$, we generate an infinite sequence recursively by

$$(K_{n+1}, |\cdot|_{n+1}, R_{n+1}, \Phi_{n+1}) = (K'_n, |\cdot|'_n, R'_n, \Phi'_n),$$

for which $|K| = |K_n|_n$ for all n . This produces an infinite sequence of mapping data (\mathcal{C}_n, f_n) , where $f_n: |K| = |K_n|_n \rightarrow \mathbb{C}$ is the discrete conformal mapping of the piecewise flat surface $|K|$ to the plane determined by the rectangular packing \mathcal{C}_n for (K_n, Φ_n) . Recall that there are four distinguished boundary vertices $\{a, b, c, d\}$ of K ordered respecting the orientation of the boundary. We assume one more normalization condition, easily accomplished by Euclidean similarities, by requiring the first two distinguished vertices a and b of K to map to the respective points 0 and 1 under each f_n , and the two others to map to the upper half plane. The image of each discrete conformal mapping f_n is then a rectangle in the upper half plane one of whose sides lies along the unit interval $[0, 1]$.

The main convergence result of [4] may be used to prove, in the special case of tangency packings where $|\cdot|$ gives a unit length to each edge, R is identically $1/2$, and Φ_R is identically 1, that the sequence of mappings $f_n: |K| \rightarrow \mathbb{C}$ exists and converges uniformly to the unique conformal mapping F of $|K|$ to a rectangle in the plane with $F(a) = 0$, $F(b) = 1$, and $F(c)$ and $F(d)$ in the upper half plane. Moreover, the pointwise quasi-conformal dilatations of the maps f_n are bounded above and converge uniformly to unity on compact subsets of the complement of the vertices of $|K|$. Our analysis of the proof will show in the next section that this holds in the piecewise flat case when R can be chosen so that Φ_R has values in the unit interval, and our goal is to understand precisely what is lacking in extending the proof to the general case.

When the sequence f_n does converge to the expected conformal map F , the conformal modulus of the conformal quadrilateral $|K|$ is thus determined to be $\mu = |F(d)|$, the height of the image rectangle $F(|K|)$. One might expect then that the maximum quasi-conformal dilatations of the sequence f_n converge to unity, but this is not the case. In fact, the maximum quasi-conformal dilatations of the sequence are in general bounded away from unity since, at any vertex v of K whose angle sum Θ determined by $|\cdot|$ is different from 2π , there is always high distortion at the vertices of K_n neighboring v ; see [4]. Nonetheless, this high local distortion is relegated to smaller and smaller neighborhoods of the original vertices of K as we progress along the sequence f_n . The result is that the limit mapping F has local dilatation 1, i.e., is conformal, at every point of $|K|$ other than those of the original vertex set \mathbf{V} . Removability of isolated singularities then comes into play to guarantee that the dilatations at the original vertices are 1 and, therefore, the limit mapping F is conformal.

4 Proving Convergence and Conformality

There are three main problems associated with the inversive distance scheme for approximating the conformal mapping of $|K|$ to a rectangle. The first is that of the existence of a rectangular packing \mathcal{C}_n for (K_n, Φ_n) , the second is that of quasi-conformality of the mappings f_n with globally bounded dilatations, and the third is that of the rigidity of infinite hexagonal packings of the plane with prescribed periodic inversive distance data. The first problem concerns the existence of the approximating sequence f_n , the second concerns the convergence of the sequence f_n to a quasi-conformal mapping F , and the third concerns the conformality of the limit mapping F . We shall discuss each of these in turn after some general comments on inversive distance packings with Φ -values restricted to lie in $[0, 1]$, i.e., in which two neighboring circles intersect nontrivially. This has been the subject of a large body of theoretical research over the past decade and a half and there is an extensive literature on the subject of existence and uniqueness of packings, particularly in the tangency case where Φ is identically 1. The understanding of the existence and uniqueness of tangency circle packings with prescribed combinatorics, as well as rigidity of infinite packings, is crucial in the work of [10] and [4] where mapping algorithms are shown to converge to the correct conformal mappings. Using existence, uniqueness, and rigidity results now in place allows us to adapt the proofs of [4] to the nontangency but overlapping case where Φ may take values in the interval $[0, 1]$. This section will give just such a proof that also covers the general case of unrestricted Φ values if the three problems that we analyze in this section are found to have appropriate resolutions.

The problem of existence. The existence and uniqueness of tangency circle packings for a complex K was first proved in [2] for arbitrarily assigned boundary radii or angle sums. This is viewed in [2] as the discrete analogue of the classical Perron method of solving the Dirichlet Problem on planar domains. Existence and uniqueness results for overlapping packings with prescribed angles of overlap, where Φ has values in the unit interval, are proved in [12] and [6]. It follows from this work that a rectangular packing for the data (K_n, Φ_n) exists as long as the values of Φ_n lie in the unit interval and two technical conditions first described by Thurston in [12] are satisfied. These *Thurston conditions* are, for an inversive distance assignment Φ ,

- T1 If a simple loop in the complex K formed by the three edges e_1, e_2, e_3 separates the vertices of K , then $\sum_{i=1}^3 \cos^{-1} \Phi(e_i) < \pi$;
- T2 If $v_1, v_2, v_3, v_4 = v_0$ are distinct vertices of K forming edges $\langle v_{i-1}, v_i \rangle$ and $\Phi(\langle v_{i-1}, v_i \rangle) = 0$ for $i = 1, 2, 3, 4$, then either $\langle v_0, v_2 \rangle$ or $\langle v_1, v_3 \rangle$ is an edge of K .

The problem of existence persists when neighboring circles are allowed to be disjoint, where the Φ values may be greater than unity. In this case the general boundary value problem is not always solvable, i.e., there are examples of inversive distance assignments Φ where no circle packing in the plane with the combinatorics of K can realize the inversive distance data. Even when such packings do exist, they may not exist with predetermined boundary radii or angle sums. Thus, there are examples of data (K, Φ) for which there are no rectangular packings. These will be detailed in forthcoming publications, but for now their existence points to the fact that the moduli space of data for which there do exist general inversive distance packings is a much more complicated object than those for the special cases of tangency and overlapping packings.

For the present work, this lack of a complete understanding of the existence of a circle packing for (K, Φ) means that we cannot guarantee that the seed packing \mathcal{C}_0 for our algorithm exists. However, when it does exist, the algorithm produces a sequence of approximate conformal mappings. The examples of inversive distance packing data without rectangular packings require some gymnastics to construct and do not seem to arise naturally from, for example, polyhedral surfaces embedded in \mathbb{R}^3 . We have never encountered a surface in practice where the lack of existence prevented us from building a seed packing for the algorithm. This problem does not seem to be a major practical impediment to the widespread application of the inversive distance scheme for conformally mapping piecewise flat surfaces to the plane.

The problem of quasi-conformality. Assume the rectangular packings \mathcal{C}_n , and therefore the discrete conformal mappings f_n , exist for all n . The argument of [4] for proving convergence of f_n to a limit mapping F in the tangency case uses the classical theory of normality of families of quasi-conformal mappings found, for instance, in [9]. The argument, which is given for conformal

quadrilaterals in the proof of the theorem below, requires that f_n be a sequence of quasi-conformal mappings with *bounded dilatations*, meaning that there is a global bound κ on the maximal dilatations $\kappa(f_n)$ of all the maps in the sequence. In this case, it will be shown that the sequence f_n converges uniformly to a κ -quasi-conformal mapping of $|K|$.

Quasi-conformality of each map f_n as well as a global bound on their dilatations in the tangency case is guaranteed by the ring lemma of [10]. Forthcoming publications will show that the ring lemma generalizes to those inversive distance packings for which Φ never takes the value 0, i.e., the case of non-orthogonal overlaps, and for which the Thurston conditions hold. However, this generalized ring lemma provides quasi-conformality only in the overlapping case where the Φ values lie in the half-closed interval $(0, 1]$. The lemma does not provide quasi-conformality in the setting of disjoint circle neighbors where Φ may take values greater than unity. In fact, there are examples of inversive distance assignments given by Φ where \mathcal{C} exists, so that the discrete conformal mapping f exists, for which f is not quasi-conformal. Thus there is no guarantee that even if the sequence f_n exists that each mapping is quasi-conformal, and even if each is, there is no guarantee that the sequence has bounded dilatations. Again these examples require some gymnastics to construct and seem not to appear among, for example, polyhedral surfaces in \mathbb{R}^3 , and again this problem does not seem to be a major practical impediment to the widespread application of the inversive distance scheme.

The problem of rigidity of infinite hexagonal packings. Assume now that the first two problems have been resolved for $|K|$ and we have a sequence of discrete conformal mappings f_n , each quasi-conformal, with dilatations bounded by κ . In this case there will exist a κ -quasi-conformal limit mapping F . The final step for uniformizing $|K|$ is the verification of the conformality of F . This step is accomplished for tangency packings in both [10] and [4] by use of the hexagonal packing lemma of [10], which depends on a rigidity result about infinite circle packings of the complex plane. The analogous rigidity result for overlapping packings is proved in [6], and so the ingredients are in place to verify conformality of the limit mapping whenever Φ takes values in the unit interval. We believe that a very general rigidity result holds for arbitrary locally finite inversive distance packings of the complex plane, but for the proof of conformality, all we need is the verification of the following specialized rigidity conjecture. In the conjecture, H is the constant 6-degree triangulation of the plane. The edges of H may be put into three equivalence classes depending to which edge of a fixed face τ a given edge is “parallel”. A circle packing of \mathbb{C} is *locally finite* provided each point of the plane has a neighborhood that meets only finitely many circles of the packing.

Conjecture 1. Let α , β , and γ be the inversive distances between respective pairs of three equi-radii circles in the plane whose centers are the vertices of

a nondegenerate triangle. Let Θ be an inversive distance edge function for H that assigns the values α , β , and γ to the three respective edges of each face so that Θ is constant on each of the three equivalence classes. Then locally finite circle packings for (H, Θ) are unique up to Euclidean similarity, i.e., if \mathcal{C} and \mathcal{C}' are both locally finite circle packings for (H, Θ) , then there is a similarity S such that $S(\mathcal{C}) = \{S(C) : C \in \mathcal{C}\} = \mathcal{C}'$.

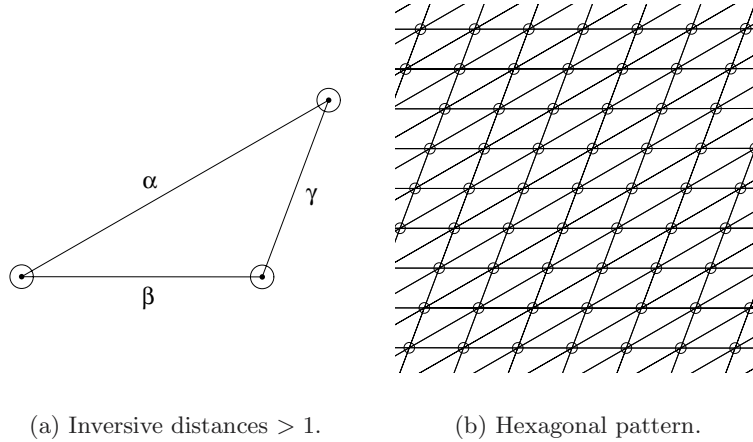


Fig. 7. Hexagonal rigidity.

If the conjecture is true, then any circle packing for (H, Θ) has $\mathbb{Z} \times \mathbb{Z}$ -symmetry with fundamental domain the union of any two triangles formed by connecting neighboring circle centers and that meet along a common edge. This follows by placing three circles of equal radii in the plane such that the pairwise inversive distances are given by α , β , and γ . The plane then may be triangulated in the hexagonal pattern with isometric copies of the triangle obtained by connecting the centers of these three equi-radii circles. An example where $\alpha = 113.0346$, $\beta = 51.8889$, and $\gamma = 31$ appears in Fig. 7.

When each of α , β , and γ are no greater than unity, results of [6] verify the conjecture. The next theorem shows how normality of a quasi-conformal family with bounded dilatations and the conjecture are used to prove conformal convergence. We make the restriction in the theorem and its corollary that Φ never takes the value 0 so that the circle packings have no orthogonal neighboring circles.

Theorem 1. *If the sequence of discrete conformal mappings f_n exists, is quasi-conformal with bounded dilatations, and Conjecture 1 holds, then f_n converges uniformly on compact subsets of the interior of $|K|$ to a conformal mapping F of $|K|$ to a rectangle in the complex plane with $F(a) = 0$,*

$F(b) = 1$, and $F(c)$ and $F(d)$ in the upper half plane. Moreover, the maximum dilatation of f_n converges to unity uniformly on compact subsets of the complement of \mathbf{V} in $|K|$.

Proof. Suppose the hypotheses hold so that f_n is a sequence of quasi-conformal mappings of $|K|$ to the plane with a global bound κ on the quasi-conformal dilatations. Let μ be the conformal modulus of the conformal quadrilateral $|K|$ and let $F: |K| \rightarrow \mathcal{R}$ be the unique conformal mapping from $|K|$ to the rectangle in the plane with vertices $0, 1, \mu i$ and $F(a) = 0, F(b) = 1, F(c) = 1 + \mu i$, and $F(d) = \mu i$. As F is 1-quasi-conformal, each of the mappings $f_n \circ F^{-1}$ is κ -quasi-conformal. Theorem II 5.1 of [9] applies to show that the family of κ -quasi-conformal mappings $\mathcal{F} = \{f_n \circ F^{-1}: n = 1, 2, \dots\}$ is normal in the interior of \mathcal{R} . Let w be any limit function of a sequence from \mathcal{F} , say $w = \lim f_{n(i)} \circ F^{-1}$ for a subsequence $f_{n(i)}$, where the limit is uniform on compact subsets of the interior of \mathcal{R} . By Theorem II 5.3 of [9], there are exactly three possibilities: the limit function w on the interior of \mathcal{R} is a constant mapping, a mapping onto two distinct points, or a κ -quasi-conformal mapping. We show next that the first two possibilities do not occur.

Let \mathcal{S} be the open infinite strip in the complex plane between the horizontal lines through $\pm \mu i$. Since the four corners and sides of \mathcal{R} are mapped by $f_n \circ F^{-1}$ to the four corners and sides of the image rectangle $\mathcal{R}_n = f_n(|K|)$, the reflection principle for quasi-conformal mappings [9] may be iterated to produce a κ -quasi-conformal extension F_n of $f_n \circ F^{-1}$ to the domain \mathcal{S} , as well as a κ -quasi-conformal extension \tilde{w} of w . Since w is a limit function of a sequence from \mathcal{F} , \tilde{w} is a limit function of a sequence from $\tilde{\mathcal{F}} = \{F_n: n = 1, 2, \dots\}$. By Theorem II 5.3 of [9], there are exactly the same three possibilities for this function \tilde{w} . Notice though that \tilde{w} is the identity on the set of integers, which are contained in the interior of \mathcal{S} , so the first two possibilities are ruled out. It follows that \tilde{w} is a κ -quasi-conformal mapping and, as w is the restriction of \tilde{w} to \mathcal{R} , so too is w .

The carrier \mathcal{R}_n of \mathcal{C}_n is a rectangle in the upper half plane with one side the unit interval. Theorem II 5.4 of [9] implies that the image of w is the kernel of the interiors of the rectangles $\mathcal{R}_{n(i)}$, and it is easy to see that such a kernel must be a rectangle with one side the unit interval. We show below that w is conformal, which immediately implies that this image rectangle $w(\mathcal{R})$ must be \mathcal{R} itself and that w must be the identity mapping of \mathcal{R} since it fixes the four corners. It follows that $f_{n(i)}$ converges uniformly on compact subsets of the interior of $|K|$ to F , the unique conformal mapping of $|K|$ to \mathcal{R} with $F(a) = 0$ and $F(b) = 1$. As w is an arbitrary limit function of a sequence from \mathcal{F} , this argument shows that there is only one such limit function, namely, the identity function on \mathcal{R} . As the collection \mathcal{F} is a normal family of mappings, so that every infinite subset of \mathcal{F} has a limit function, it follows that the sequence $f_n \circ F^{-1}$ itself converges uniformly on compact subsets of the interior of \mathcal{R} to this identity function, or that the sequence f_n converges uniformly on compact subsets of $|K|$ to F . This completes the

proof of convergence of the f_n to a conformal mapping of $|K|$ modulo the verification that w is in fact conformal. This will be accomplished next with the aid of Conjecture 1.

Let α, β, γ, H , and Θ be as in Conjecture 1 and for each n , let H_n be the subcomplex of H formed by n generations of the hexagonal grid about some fixed vertex v_0 . Let $\sigma = \langle v_0, v_1, v_2 \rangle$ be a face of H containing v_0 and let Θ_n be the restriction of Θ to the edges of H_n . A proof using the rigidity of Conjecture 1 and the generalized ring lemma, similar to the proof of the hexagonal packing lemma of [10], shows that there is a sequence ε_n decreasing to zero such that, if \mathcal{H}_n is any oriented circle packing for (H_n, Θ_n) , and if τ_n is the triangle in \mathbb{C} formed by connecting the centers of the circles in \mathcal{H}_n corresponding to v_0, v_1 , and v_2 and τ is the triangle formed by connecting the centers of the circles in the unique packing \mathcal{H} corresponding to v_0, v_1 , and v_2 , then the vertex preserving affine map from τ_n to τ has dilatation at most $1 + \varepsilon_n$. This is a very strong statement concerning the shapes of the triangles τ_n as the constants ε_n do not depend on which packing for (H_n, Θ_n) is chosen, but merely on the fact that v_0 is “ n -deep” within the complex H_n .

Let D be a compact subset contained in an open face σ of $|K|$. Let N be an arbitrary positive integer and choose n so large that each point z of D is centered in a simply connected neighborhood U_z formed by N generations of the hexagonal grid in $|K_n|$ that results from n hex-refinements of the face σ . The generalization of the hexagonal packing lemma of the previous paragraph guarantees that f_n has maximum dilatation at most $1 + \varepsilon_N$ on D , and since ε_N decreases to zero, the maximum dilatation converges to unity uniformly on D . This implies by Theorem II 5.3 of [9] that the dilatation of the limit mapping F at any point in the interior of a face of K is no more than $1 + \varepsilon_N$, for all N , and therefore F is conformal on the interiors of the faces of K . By removability of analytic arcs and isolated singularities, F is conformal on $|K|$. We emphasize here that this argument with the use of the generalized hexagonal packing lemma requires that our radius function R , from which the seed inversive distance function Φ_0 is calculated, be constant on the vertex set \mathbf{V} . One may run the algorithm with arbitrary variable radius function R , but the convergence generally will not be to a conformal mapping.

The last statement of the theorem requires a small modification to show uniform convergence when the compact set D hits edges, which we shall not present. \square

Corollary 1. *If all the edge lengths $|e|$ lie in the half-close interval $(\lambda, \sqrt{2}\lambda]$, for some positive constant λ and the Thurston conditions (T1) and (T2) hold, then the functions f_n exist and are quasi-conformal with bounded dilatations, and the sequence converges uniformly on compact subsets of the interior of $|K|$ to a conformal mapping F of $|K|$ to a rectangle in the complex plane with $F(a) = 0$, $F(b) = 1$, and $F(c)$ and $F(d)$ in the upper half plane. Moreover, the maximum dilatation of f_n converges to unity uniformly on compact subsets of the complement of \mathbf{V} in $|K|$.*

Proof. If the initial radius function R_0 is chosen to have constant value $\lambda/\sqrt{2}$, then the initial inversive distance edge function Φ_0 takes values in the half-closed interval $(0, 1]$, since all the edge lengths $|e|$ lie in the interval $(\lambda, \sqrt{2}\lambda]$. Notice that the values of each Φ_n are the same as those for the initial inversive distance edge function Φ_0 , so that the Φ_n values are in the unit interval. Thus the circle packings \mathcal{C}_n are either tangency or nonorthogonal overlapping packings. The sequence f_n exists by existence-uniqueness results of [2] and [6] that cover the tangency and overlapping packing cases. Quasi-conformality of the f_n with bounded dilatations follows from the ring lemma of [10] for the tangency case and its generalization for the overlapping case. The verification of Conjecture 1 for the tangency case appears in [10] and for the overlapping case in [6]; see also [11]. Theorem 1 applies. \square

5 A Gallery of Quadrilaterals

Example 1. Our first examples are those of Figs. 1 and 2. In Fig. 1(a) all edges have unit length and the surface $|K|$ is an equilateral surface formed by gluing eight unit equilateral triangles along edges that meet at a common central vertex. By conformal symmetry at the central vertex, the central angles of all the triangles have measure $\pi/4$ in the conformal structure though they all have Euclidean measure $\pi/3$ in the piecewise flat structure. Notice that there are anti-conformal reflections across the diagonals from a to c through the center and from b to d through the center, as well as across the other two diagonals. Thus the dihedral group D_4 , the symmetry group of the square, acts as a group of conformal symmetries of $|K|$. The only rectangles on which D_4 acts conformally are squares, so we know before running the inversive distance scheme that the conformal modulus of $|K|$ is 1 and $|K|$ is conformally equivalent to a square via a mapping taking the equilateral faces to congruent $(2, 4, 4)$ triangles formed by the diagonals and opposite edge bisectors of a square. `CirclePack` confirms this in Fig. 2(a). Since this is an equilateral surface, we used tangency packings with unit inversive distance function.

In Fig. 1(b) all edges have unit length except for the three boundary edges labeled by γ , each of which has edge length $\gamma = 2 \sin \frac{\pi}{18} \approx 0.3473$. This makes the Euclidean angles opposite γ equal to $\pi/9$ so that the total Euclidean angle spanned opposite the three labeled sides is $\pi/3$, the same as the Euclidean angles of the equilateral triangles at that vertex. The total Euclidean angle sum around the central vertex is 2π , so the angles measured by the conformal structure at the central vertex agree with the Euclidean measures. In particular, a conformal mapping to a rectangle will map the faces so that the Euclidean angles at the central vertex are preserved. Again `CirclePack` confirms this in Fig. 2(b). This time the rectangle is not a square and the conformal modulus of the conformal quadrilateral $|K|$ is $\mu = 1.2031$. The fixed value we chose for the radius function R , from which the inversive

distance edge function Φ is calculated by Equation 3, is $\gamma/2$. This makes the inversive distance values unity along the γ edges and 15.5817 otherwise.

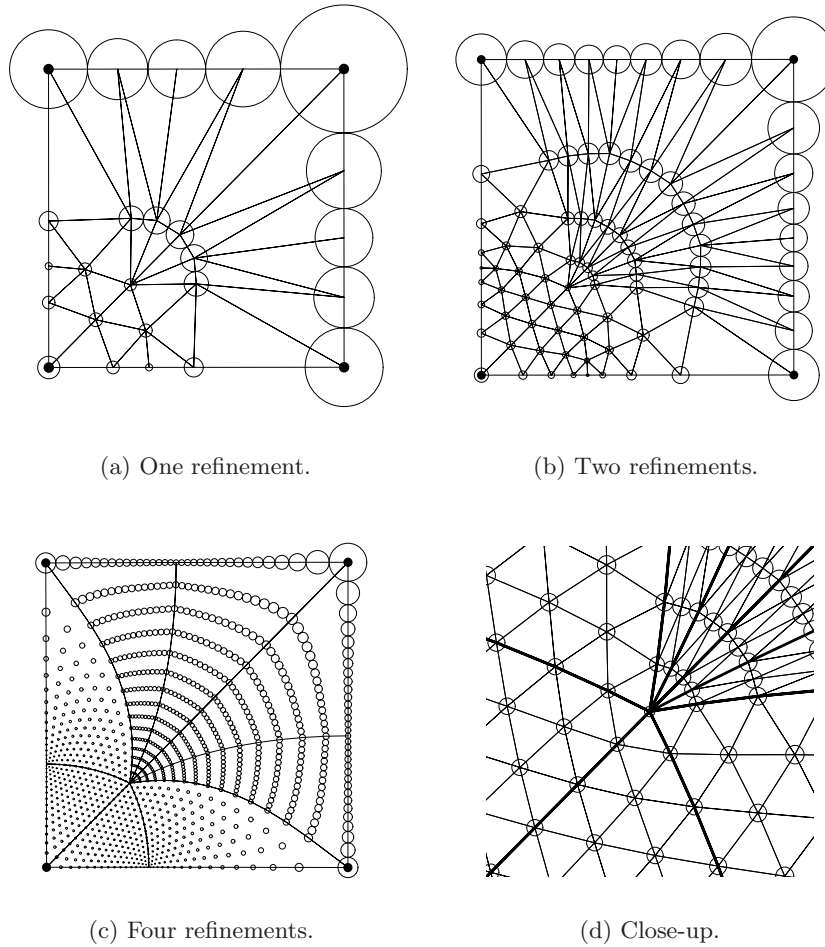


Fig. 8. Converting to conformality.

In Fig. 1(c) all edges have unit length except for the four boundary edges labeled by δ , each of which has edge length $\delta = 2 \sin \frac{\pi}{24} \approx 0.26105$. This makes the Euclidean angles opposite δ equal to $\pi/12$ so that the total Euclidean angle spanned opposite the four labeled sides is $\pi/3$. Thus the market share of these four angles totaled equals the market share of each of the other angles at the central vertex in the unit equilateral triangles. This means that the conformal structure on $|K|$ measures the total angle spanned opposite

the four labeled sides as $2\pi/5$ as well as the remaining four angles at the central vertex in the four equilateral triangles. In particular, the conformal structure measures each angle opposite δ as $\pi/10$ though the Euclidean measure is $\pi/12$. Also, $|K|$ has an anti-conformal reflection across the diagonal from a to c and, since squares are the only rectangles with a diagonal conformal symmetry, we know that the conformal modulus of $|K|$ is 1 and $|K|$ is conformally equivalent to a square. Again `CirclePack` confirms this in Fig. 2(c). The fixed value we chose for the radius function R is $\delta/2$, which makes the inversive distance values unity along the δ edges and 28.3477 otherwise. Fig. 8 shows the image rectangular packings at stages one, two, and four of the inversive distance iteration, with only the image of the original triangulation shown for the fourth stage packing, as well as a close-up of the central vertex from the stage four refinement.

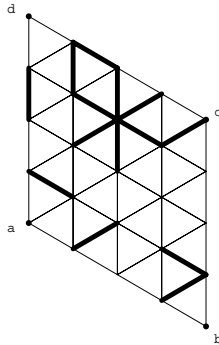


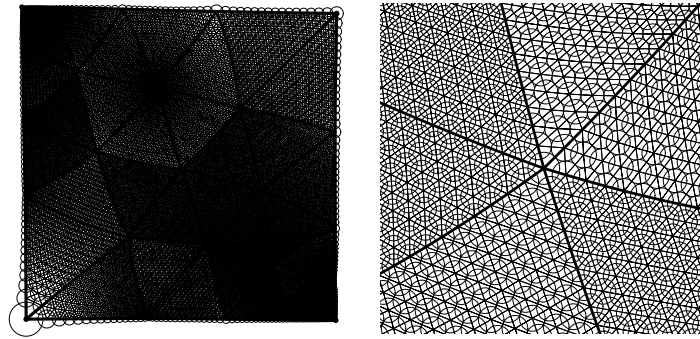
Fig. 9. Hexagonal grid: lengths of bold edges are 1.1; others are 1.4.

Example 2. The edge length assignments used in Fig. 9 for the complex K have $|e|$ equal to 1.1 for the bold edges and 1.4 otherwise. We approximate the conformal mapping of $|K|$ to a rectangle using three different choices for the initial radius function. The radius function $R(1)$ takes the constant value $1/\sqrt{2}$ where all neighboring circles overlap nontrivially. The second $R(2)$ takes the constant value $3/5$ where there is a mixture of overlapping and disjoint circles in the initial configuration. The third $R(3)$ takes the constant value $1/4$ where all circle pairs are disjoint. The inversive distance algorithm with any of the three seed radii should provide approximations that converge to the unique conformal mapping of $|K|$ to a rectangle of unit horizontal side length. Fig. 10 shows the fourth iterate of the inversive distance scheme applied with each of the three seed radii functions. The circle packings themselves with the images of the edges of the initial triangulation K darkened are shown, along with a close-up of a neighborhood of one of the vertices. This experimentation with `CirclePack` suggests that the convergence is independent of the initial

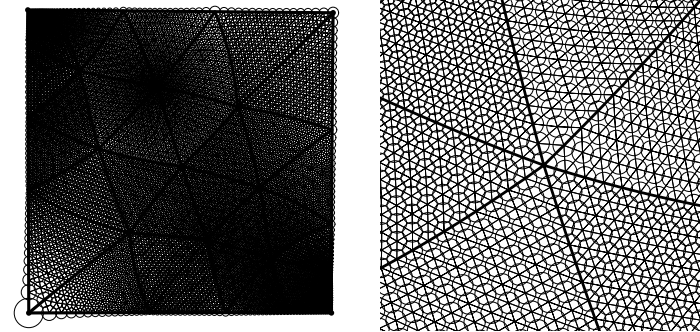
constant radius value, as it should be. The ranges of the Φ values are 0.2100 to 0.9600 for $\Phi_{R(1)}$, 0.6806 to 1.7222 for $\Phi_{R(2)}$, and 8.6800 to 14.6800 for $\Phi_{R(3)}$.

Example 3. Corollary 1 confirms that the inversive distance scheme converges in case the piecewise flat metric is *equilateral*, i.e., when the edge length function $|\cdot|$ takes the constant value 1. Then the metric surface $|K|$ is a union of equilateral triangles glued side-to-side and, when the radius function R takes the constant value $1/2$, the inversive distance function Φ_R takes the constant value 1. The rectangular packings are then tangency packings. Fig. 11 shows three examples of piecewise equilateral quadrilaterals and their uniformizations as rectangles. Each edge in the left-hand figures is given unit length, and four refinements are used to approximate the rectangular uniformizations on the right. An interesting feature of equilateral surfaces is that they have a *reflective* structure in which each face reflects across any interior edge to its companion face, see [4]. This reflection is an anti-conformal map and the whole surface is generated by fixing any one face and then reflecting across edges iteratively. This is obvious in the piecewise equilateral manifestation of the surface, and this translates into the following property of their rectangular conformal images. The image $\tau' = F(\tau)$ of any equilateral face τ of $|K|$ under the conformal mapping to a rectangle contains all the information about the rest of the map in the sense that the rest of the map and the image curvilinear triangulation of the rectangle can be recovered by anti-conformal reflections iterated starting with τ' . This suggests that, in principle, an arbitrary finite or even countably infinite amount of information can be represented in the shape of a single curvilinear triangle and then recovered by anti-conformal reflections. This is theoretically interesting and is illustrated in the next example.

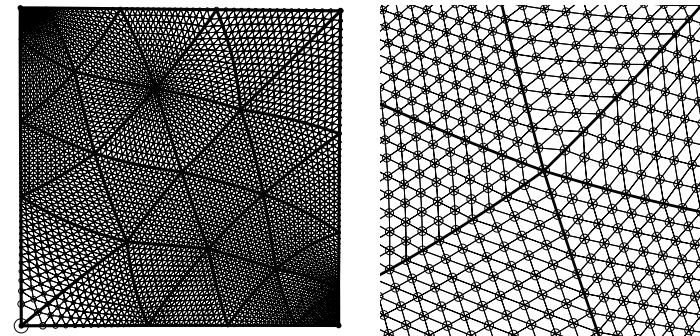
Fig. 12(a) shows an eight-by-eight square with each subsquare divided into two triangles with either a right or left slash. The right slash encodes a zero and the left a one, and the rows encode the individual symbols of the expression ‘vismath!’. The resulting triangulation is given an equilateral metric with all unit edge lengths and this surface is mapped conformally to a rectangle. The resulting reflective curvilinear triangulation is shown in Fig. 12(b) and the upper left-hand corner triangle is enlarged in Fig. 12(c). The whole triangulation in Fig. 12(b), and therefore the message ‘vismath!’, may be recovered from the lone triangle in Fig. 12(c) (or from any other triangle in the figure) by iterated anti-conformal reflection. Of course there is nothing to restrict our attention to finite triangulations. We might well triangulate the plane, prescribe that each face be a unit equilateral triangle, then conformally map the resulting piecewise equilateral surface to the plane \mathbb{C} or to the unit disk. The image of any face then contains all the combinatorial information of the original triangulation. The interested reader might find the discussion of [3] enlightening.

(a) $R = 1/\sqrt{2}$.

(b) Close-up.

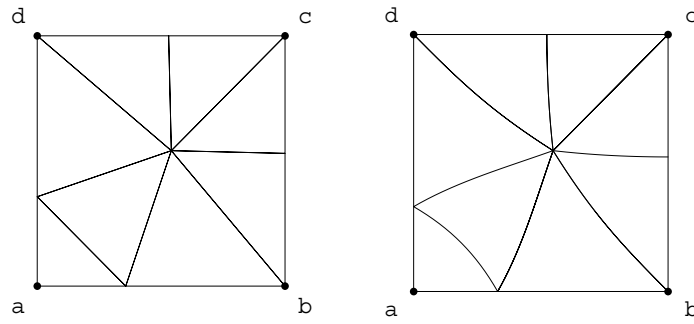
(c) $R = 3/5$.

(d) Close-up.

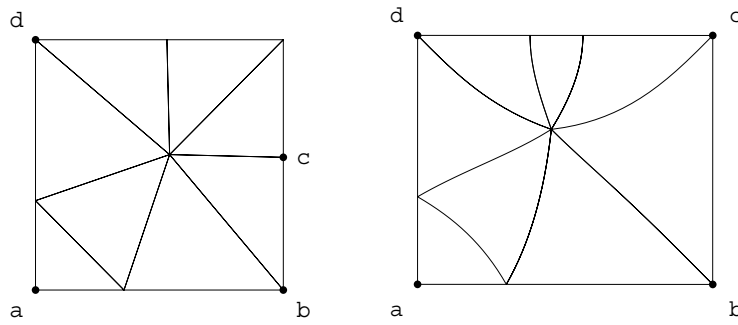
(e) $R = 1/4$.

(f) Close-up.

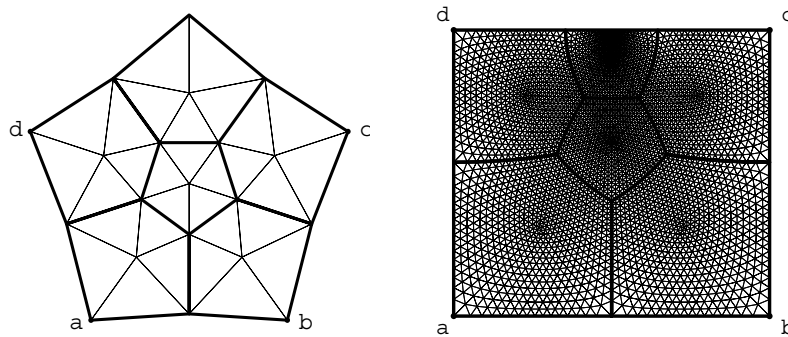
Fig. 10. Hexagonal grid.



(a) A quadrilateral and its reflective triangulation.

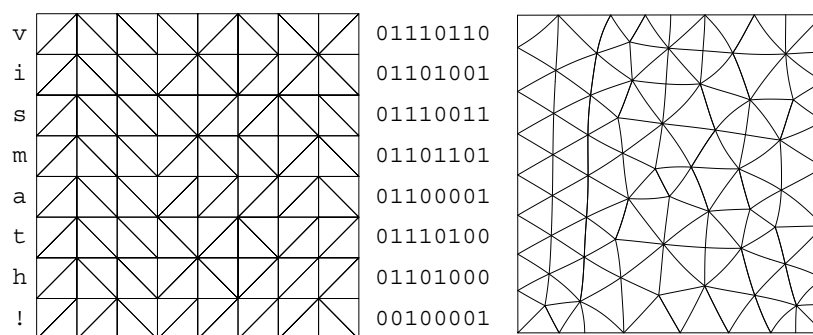


(b) A different corner point c .



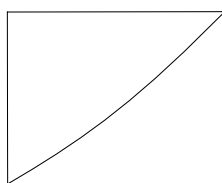
(c) A pentagonal packing and its reflective triangulation.

Fig. 11. Equilateral surfaces and their uniformizations.



(a) Binary encoding.

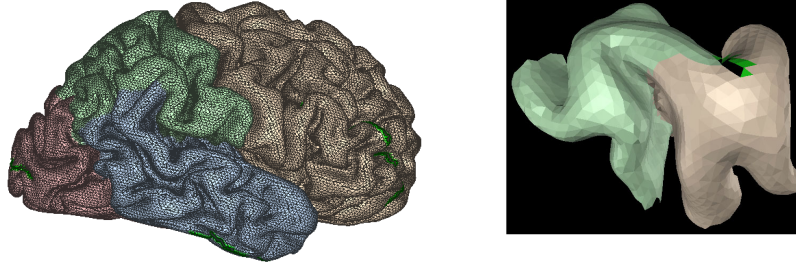
(b) Reflective encoding.



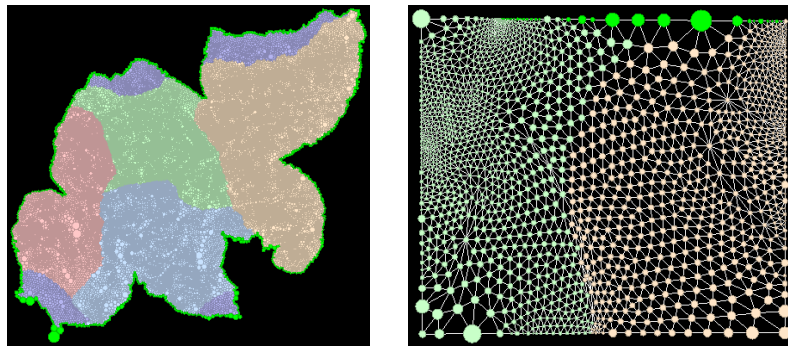
(c) Top left triangle.

Fig. 12. Encoded 'vismath!'.

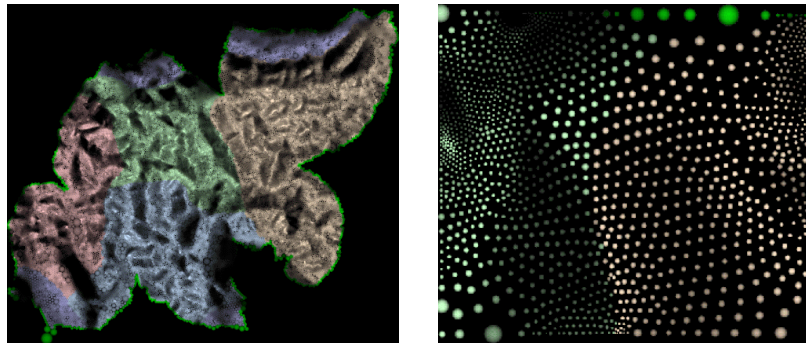
Example 4. The left-hand graphic of Fig. 13(a) (Color Plate 1(a) on page 427) shows a three-dimensional rendering of the surface of a human cerebrum obtained from the Visible Man data from the National Library of Medicine. This example contains 52,360 vertices and 103,845 faces. Hurdal *et al* [8] flattened this mesh quasi-conformally using tangency packings where all inversive distances are set to unity. They then computed a textured bump map using a fake diffuse component for each circle using the surface normal in \mathbb{R}^3 . The color for each circle was then scaled based on the diffuse value. In this way the fissures and sulci of the three-dimensional brain data can be represented in the flat mapping, see [8]. The results appear in the left-hand graphics of Figs. 13(b) and 13(c) (Color Plates 1(b) and 1(c) on page 427), where boundary data from the three-dimensional surface has been used to normalize the packing. One can see the dramatic effect bump map texturing has in these flattened images. In the right hand graphics of Fig. 13 (Color Plate 1 on page 427), we have isolated from this brain surface a quadrilateral region made up of 2943 faces with 1565 vertices, and mapped this subsurface conformally to a rectangle. We used the distances between neighboring



(a) Right hemisphere and subsurface.



(b) Radii packing of hemisphere and inversive distance packing of a subsurface.



(c) Packing with bump map texture.

Fig. 13. Quasi-conformally mapping of the human brain to a planar domain.

vertices in the three-dimensional graphic of Fig. 13(a) (Color Plate 1(a) on page 427) to compute an edge-length function $|\cdot|$ and then flattened using the inversive distance scheme. The first rectangular map, Fig. 13(b) (Color Plate 1(b) on page 427), is an inversive distance packing without the bump map texture, and the second, Fig. 13(c) (Color Plate 1(c) on page 427), is one with the bump map texture. This is a sample of ongoing work by a team of mathematicians and neuroscientists who are working to build a conformal flattening visualization tool for use in neuro-anatomical studies.

Another sample appears in Fig. 14 (Color Plate 2 on page 428) where we have conformally mapped two cerebellum images obtained from MRI scans to a disk. The top two images show the cerebellum from two different subjects. The middle two images show a mapping to a disk. The bottom two images correspond to a close-up view of the disk mapping to highlight some of the detail in the central regions of the mappings. The color coding identifies regions of interest to neuro-anatomists with the orange regions indicating areas of PET activation when the subjects perform the same tasks.

6 Implementation: Practical Experimental, Computational, and Theoretical Issues

Implementation of the inversive distance scheme for approximating conformal mappings requires the development of a computational engine that computes oriented circle packings for given inversive distance data (K, Φ) . Ken Stephenson has built such an engine in his program `CirclePack`. Its packing algorithm for tangency packings uses a refinement of Thurston's original idea in [12] as well as modern numerical schemes for fast approximation of transcendental functions. The reader may consult [5] for the latest detailed account of optimal packing algorithms. The packing algorithm generalizes to cover arbitrary inversive distance packings, though now there is no guarantee of convergence as there is in the tangency case. In fact, as we know of examples of inversive distance data (K, Φ) that have no circle packing realization, any such seed data for `CirclePack` would fail to converge. The packing algorithm is based on monotonicity results for the change in angle sums about vertices as the radius of a single circle is changed while preserving inversive distances. Again the interested reader is directed to [5] for details.

The reader might ask how practical it is to get really close approximations to the conformal mapping of $|K|$ to a rectangle since, obviously, the number of vertices grows exponentially as hex-refinement is iterated. The good news is that the experimental evidence suggests very fast convergence of the inversive distance scheme. Indeed, in all examples we have yet encountered, the difference between the fourth and fifth iteration is so small as to be unnoticeable. This points to a theoretical issue whose resolution would be very valuable for validating this experimental observation, namely, that of deriving analytic estimates on the quasi-conformal dilatations of the approximating mappings

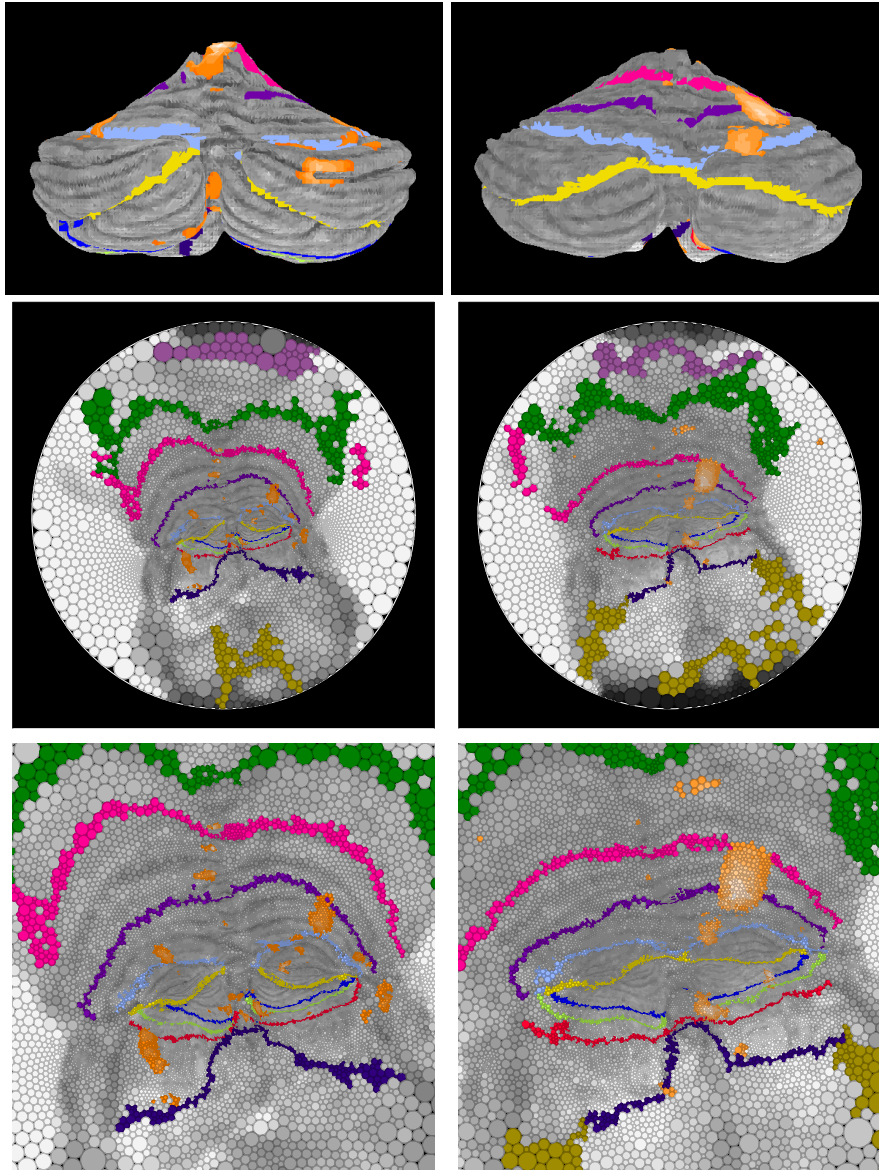


Fig. 14. Mapping two different cerebellum of the human brain.

f_n . Sharp enough estimates might explain the observed fast convergence and give an alternate, constructive proof of the convergence of the scheme. For convergence to the correct conformal mapping, the scheme requires a constant radius function for the seed, but of course an arbitrary nonconstant radius function that satisfies Inequality 2 provides inversive distance data for which a packing might exist. Good analytic bounds on dilatations might provide a method for choosing a variable radius function whose packing closely approximates $|K|$ without iteration.

It would be unwise to pretend that there are no practical implementation problems with the computational engine that computes a circle packing for given inversive distance data and with the resulting display. A particularly acute problem arises when there is a wide range of inversive distance values and the size of the complex K is large with, say, greater than 10^6 vertices. The resulting circle radii in the packing then have widely disparate values, which can lead to long computation times and numerical instabilities due to the high degree of numerical precision that is required. These large complexes, including those generated from a large number of hex refinements, can be difficult to visualize on a small computer screen. An advantage of conformal mapping for visualization of these large data sets comes into play here. Rather than map to a rectangle, we may map conformally to a disk, and then use Möbius transformations to bring various parts of the complex into focus near the disk center. This technique has proved extremely useful in developing a neuro-imaging tool.

Some improvements in the speed of the algorithm have been described by Collins and Stephenson in [5]. However there is room for considerable improvement for large data sets and for other investigations for optimizing the code. The algorithm for finding the circle packing for given inversive distance data is an iterative procedure, beginning with a specified vertex. The quasi-conformal results do not depend on the vertex chosen; however, it might be that nominating an alternate vertex would result in improved algorithm speed or faster convergence. Other computational experimental simulations may reveal additional insights into algorithm improvements. Since the algorithm is an iterative procedure, it seems to lend itself well to parallelization, which is an area of current research by Stephenson.

The computational issues described here become problems only for large complexes or data sets. For complexes such as the ones presented in this paper the algorithm is stable, robust and fast.

References

1. Beardon, A.F., (1983): *The Geometry of Discrete Groups*. Springer-Verlag, Berlin
2. Beardon, A.F., Stephenson, K. (1990): The uniformization theorem for circle packings. *Indiana U. Math. J.*, **39**, 1383–1425

3. Bowers, P.L., Stephenson, K. (1997): A “regular” pentagonal tiling of the plane. *Conformal Geom. Dynam.*, **1**, 58–86
4. Bowers, P.L., Stephenson, K. (to appear): Uniformizing dessins and Belyı̄ maps via circle packings. *Memoirs AMS*
5. Collins, C., Stephenson, K. (to appear): A circle packing algorithm. *Computational Geometry: Theory and Application*
6. He, Z-X., (1999): Rigidity of infinite disk patterns. *Ann. of Math.*, **149**, 1–33
7. Hurdal, M.K., Bowers, P.L., Stephenson, K., Sumners, D.L., Rehm, K., Schaper, K., Rottenberg, D.A. (1999): Quasi-conformally flat mapping the human cerebellum. In: Taylor, C., Colchester, A. (eds) *Medical Image Computing and Computer-Assisted Intervention–MICCAI’99*. Springer Berlin **1679**, 279–286
8. Hurdal, M.K., Kurtz, K.W., Banks, D.C. (2001): Case study: interacting with cortical flat maps of the human brain. In: *Proceedings Visualization 2001*, IEEE, Piscataway, NJ, 469–472, 591
9. Lehto, O., Virtanen, K.I., (1970): *Quasiconformal Mappings in the Plane*, 2nd ed. Springer-Verlag Berlin
10. Rodin, B., Sullivan, D. (1987): The convergence of circle packings to the Riemann mapping. *J. Diff. Geo.*, **26**, 349–360
11. Schramm, O. (1991): Rigidity of infinite (circle) packings. *J. AMS*, **4**, 127–149
12. Thurston, W. (notes): The geometry and topology of 3-manifolds. Available from Princeton U. Math. Dept.